

FIGURE S1: Comparison of TIM-3 expression in primary human T cells and virally-transduced Jurkat NF- κ B reporter cells

After 7 days of stimulation with α CD3/ α CD28, human peripheral blood mononuclear cells (PBMCs) were analyzed by flow cytometry for expression of CD3, CD8, CD4, and TIM-3. (A) Doublet discrimination was performed to select singlet PBMCs for analysis. Detected events were analyzed and gated as shown (left panel). Gated cells were assessed for their side scatter height and width (middle panel), and then forward scatter height and width (right panel) to discriminate doublets and select singlets, in gate termed "PBMC". (B-D) Analysis of CD3, CD8, CD4 expression in the PBMC population confirm that T cells were expanded during 7-day stimulation, as the majority of cells express CD3 (B, C). Approximately half of the CD3⁺ cells express CD8 or CD4, as shown in the CD3⁺CD8⁺ or CD3⁺CD4⁺ in panels (B) and (C), respectively. (D) Expression of CD8 and CD4 is mutually exclusive, as expected.

(E) TIM-3 levels on TIM-3⁺ Jurkat NF- κ B cells (red) are compared to those on CD3⁺CD8⁺ PBMCs (green), CD3⁺CD4⁺ PBMCs (orange), or the bulk PBMC population (blue), as defined in the dot plots shown in **(B)**, **(C)**, and **(A, right panel)**. Unstained PBMC (blue) and TIM-3⁺ Jurkat NF- κ B cells (pink) controls are shown in dotted lines with shaded peaks.

(F) Parental (black) and TIM-3⁺ (red) Jurkat reporter cells were stimulated with α CD3 (1 μ g/ml) only, to assess whether the co-stimulatory effect of TIM-3 can be observed with CD3 engagement only. Relative MFI of the GFP reporter was quantified and normalized to the parental MFI for each stimulation. A representative histogram is shown at the left, and quantitation of relative mean GFP fluorescence intensity (MFI) from two independent biological repeats (mean \pm SD) is shown at right.

(G) Companion experiments for **(F)**, in which parallel stimulations were performed with both α CD3 (1 μ g/ml) and α CD28 (0.5 μ g/ml) in combination. Relative MFI of the GFP reporter was quantified and normalized to the parental MFI for each stimulation. A representative histogram is shown at the left, and quantitation of relative mean GFP fluorescence intensity (MFI) from two independent biological repeats (mean \pm SD) is shown at right.

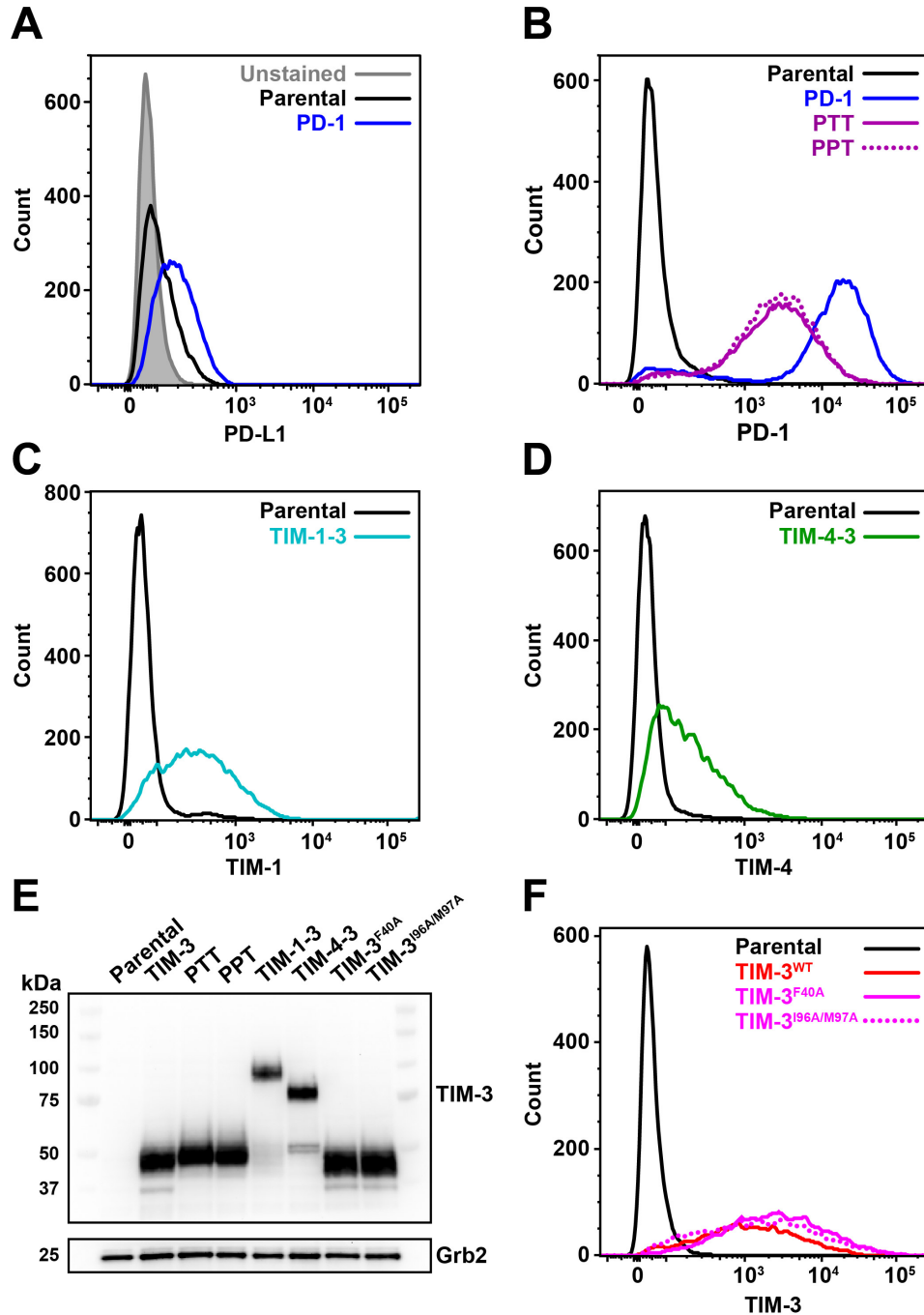


FIGURE S2: Expression of receptors in Jurkat cells after lentiviral transduction

(A) NF- κ B GFP transcriptional reporter Jurkat cells were analyzed for PD-L1 expression by flow cytometry. Parental (black curve) or PD-1-expressing (blue curve) cells were stained with fluorescently labeled anti-PD-L1 and compared to unstained PD-1-expressing cells (gray shaded).

(B) Parental NF- κ B reporter Jurkat cells do not express detectable levels of PD-1. Lentivirus transduction was used to exogenously express PD-1 or the PD-1/TIM-3 chimerae (PTT and PPT) in NF- κ B reporter Jurkat cells. Surface receptor expression was confirmed by staining with fluorescently labeled anti-PD-1, with representative histograms shown.

(C, D) Jurkat cells do not express TIM-1 (C) or TIM-4 (D), but do express the chimeric TIM-1-3 (cyan curve in (C)) and TIM-4-3 (green curve in (D)) chimerae when introduced by lentiviral transduction.

(E) Expression levels for chimeric receptors and mutated TIM-3 variants directed by transfected lentivirus in NF- κ B reporter Jurkat cells are similar to that seen for full-length, wild-type TIM-3, as assessed by Western blotting with an antibody against the intracellular region of TIM-3.

(F) Mutated TIM-3 variants with defective PS binding (TIM-3^{F40A} and TIM-3^{I96A/M97A}) were robustly expressed at the cell surface following lentiviral transduction, as detected by staining with anti-TIM-3 and labeled anti-goat antibody to ensure staining of all TIM-3 variants. TIM-3^{WT} is shown as a red curve, TIM-3^{F40A} as solid magenta curve, and TIM-3^{I96A/M97A} as dotted magenta curve.

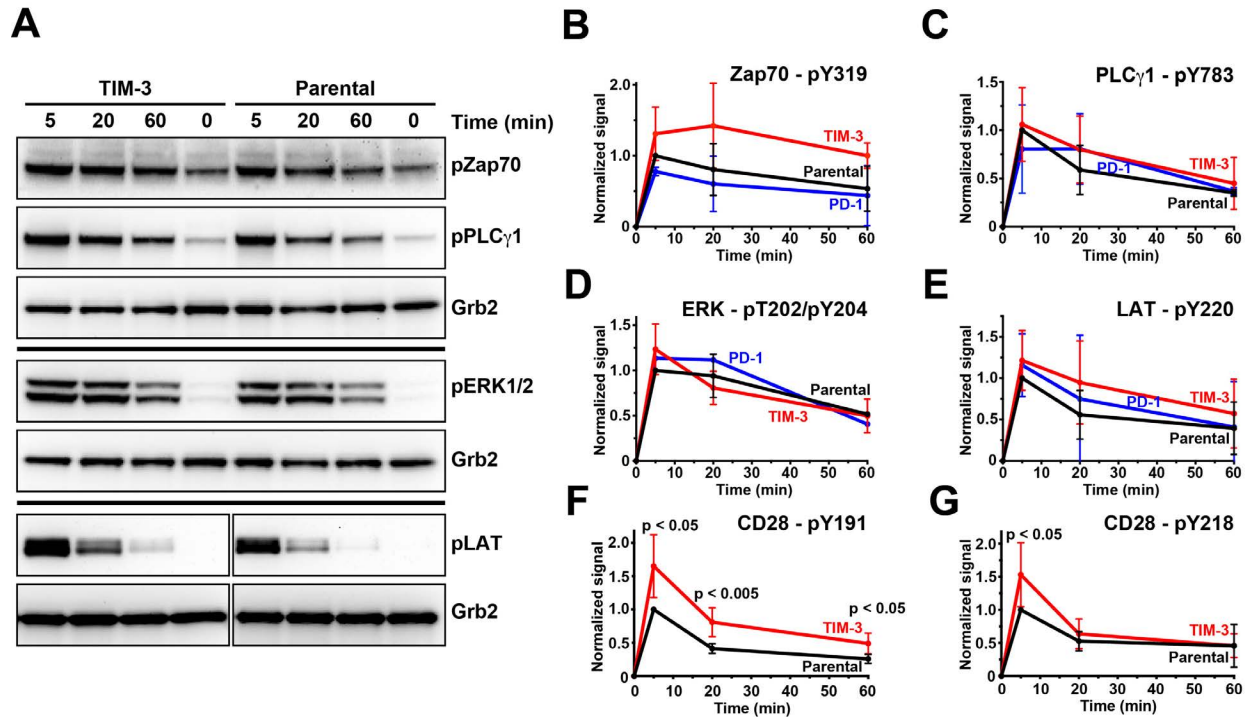


FIGURE S3: Effects of TIM-3 expression on phosphorylation of TCR signaling components

Western blotting was used to monitor changes in phosphorylation of TCR-associated signaling molecules following TCR activation.

(A) Representative Western blot with phospho-specific antibodies for Zap70 (pY319), PLC γ 1 (pY783), ERK1/2 (pT202/pY204), and LAT (pY220), with Grb2 as a loading control, for TIM-3-expressing cells (left four lanes) and parental NF- κ B reporter Jurkat cells (right four lanes).

(B-E) Band intensities for (B) phospho-Zap70 (pY319), (C) phospho-PLC γ 1 (pY783), (D) phospho-ERK1/2 (pT202/pY204), (E) phospho-LAT (pY220) are shown after 5, 20, and 60 min of stimulation, quantified using the Kodak ImageStation and normalized to Grb2 for parental NF- κ B GFP reporter Jurkat cells (black), or those expressing TIM-3 (red) or PD-1 (blue). Cells were starved for 4 h, and then stimulated with 1 μ g/ml α CD3 plus 1 μ g/ml α CD28. Data points for Zap70, LAT, and PLC γ 1 represent mean values for at least 3 independent experiments (2 for PD-1). Data points for pERK1/2 represent mean values for 2 independent experiments for parental and TIM-3 cells and 1 experiment for PD-1. Error bars show standard deviation. Statistical analysis with two-tailed, unpaired Student's t-test to compare values for TIM-3 and PD-1 cells to parental cells showed no significant differences at any time point.

(F-G) Quantification of CD28 pY191 (F) and pY218 (G) levels, with representative blots shown in **Figure 2A,B**, for 5, 20, and 60 min of stimulation. Bands were quantified using the Kodak ImageStation and normalized to Grb2 loading control. Points represent the average of 5 repeats for each phosphosite with standard deviation shown in error bars. p values comparing TIM-3 and parental cells were determined with a two-tailed, unpaired Student's t-test.

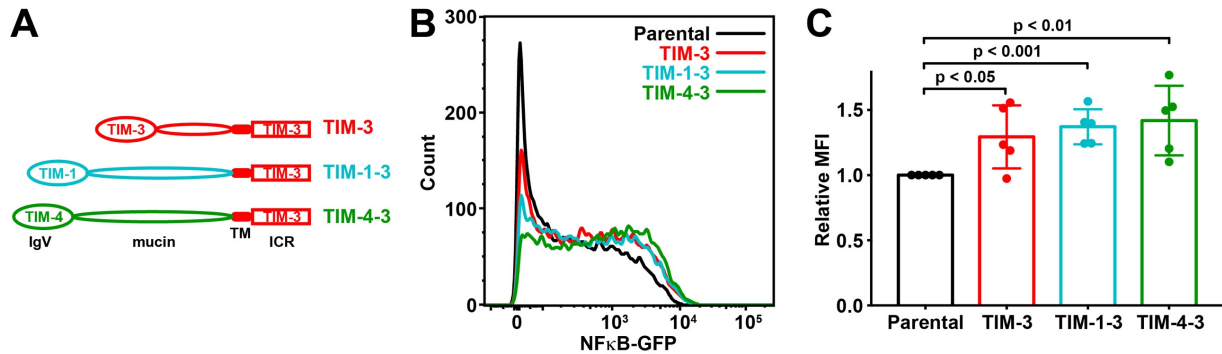


FIGURE S4: Chimeras with PS-binding TIM-1 or TIM-4 extracellular regions retain ability to promote T cell signaling

(A) Schematic representation of TIM-1/TIM-3 and TIM-4/TIM-3 chimeric constructs in which the TIM-3 ECR has been replaced with that from TIM-1 (TIM-1-3) or TIM-4 (TIM-4-3).

(B) A GFP reporter was used to measure NF-κB transcriptional activity downstream of TCR activation in parental NF-κB GFP reporter Jurkat cells (black), and those expressing wild-type TIM-3 (red), the TIM-1-3 chimera (teal), or the TIM-4-3 chimera (green) following TCR stimulation with 1 μg/ml αCD3 plus 0.5 μg/ml αCD28 for 16 h. Representative histograms of NF-κB-driven GFP expression are shown.

(C) Relative mean GFP fluorescence intensity (MFI) values, as fold change over parental cells in each experiment, is plotted for 5 biological repeats of the experiment shown in (E). Bars represent mean ± SD, with p values determined by two-tailed, unpaired Student's t-test.

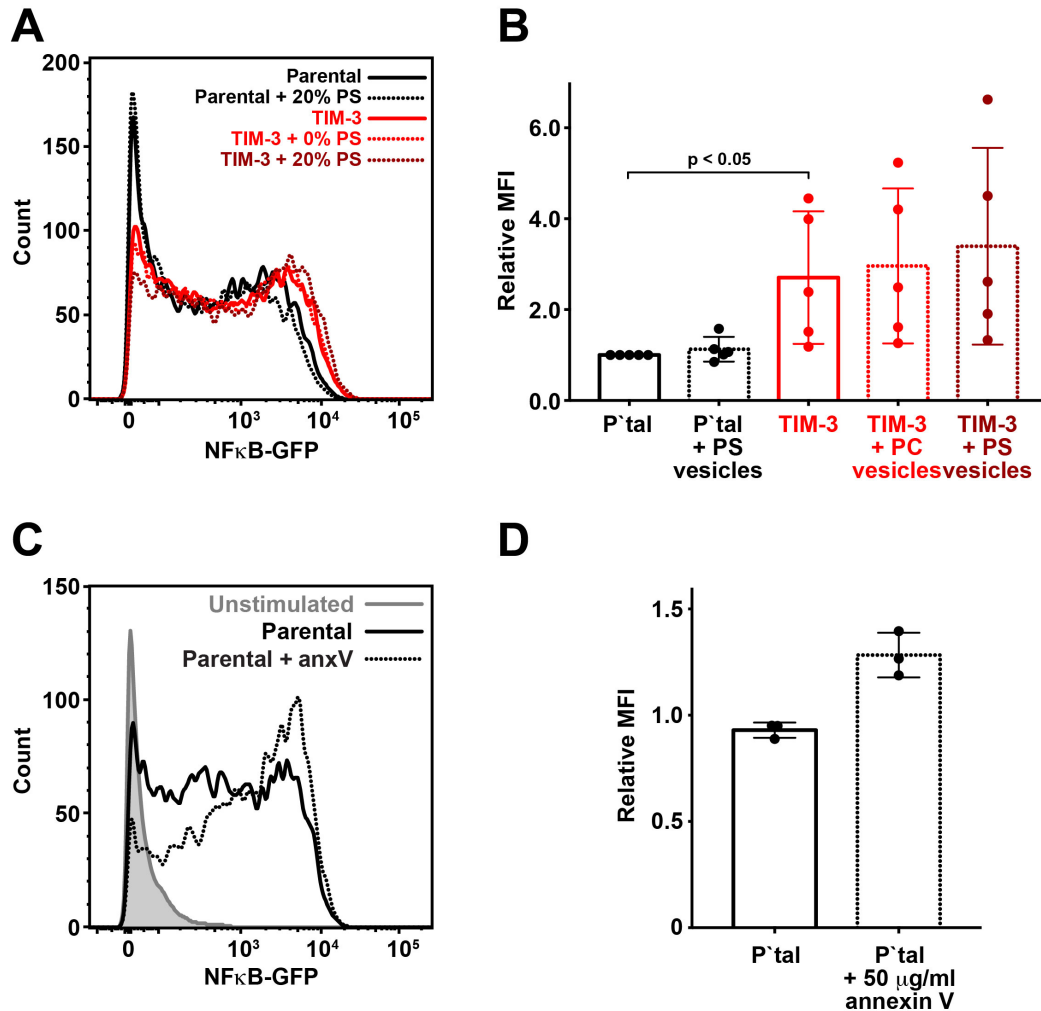


FIGURE S5: Addition of exogenous PS fails to increase NF-κB-signaling in TIM-3⁺ cells

(A) Representative histograms of NF-κB-driven GFP expression in parental NF-κB GFP reporter Jurkat cells (solid black curve) that had been serum starved for 4 h, and then stimulated with 1 μg/ml αCD3 plus 0.5 μg/ml αCD28 for 16 h. Equivalent experiments were performed in parallel with these parental cells treated with 100 μM 20% DOPS/80% DOPC vesicles (black dotted curve), TIM-3-expressing cells (red solid curve), TIM-3-expressing cells treated with 100 μM 100% DOPC vesicles (red dotted curve), and TIM-3-expressing cells treated with 100 μM 20% DOPS/80%DOPC vesicles (dark red dotted curve). Vesicle addition to TIM-3-expressing cells has no significant influence, as quantitated across experiments in (B).

(B) Quantitation of relative mean GFP fluorescence intensity (MFI) from repeats of the experiments in (A), showing substantial spread in the data, but no significant difference between treatments across 5 independent repeats. Bars represent mean ± SD.

(C) Representative histograms of NF-κB-driven GFP expression in unstimulated (gray, shaded) and stimulated parental NF-κB GFP reporter cells alone (black, solid line) or with 50 μg/ml annexin V (anxV) (black, dotted line), showing that annexin V promotes GFP expression in this system even in stimulated parental cells.

(D) Quantitation of data in (C), comparing parental (P'tal) cells with- and without annexin V. Mean ± SD is shown for biological triplicate.

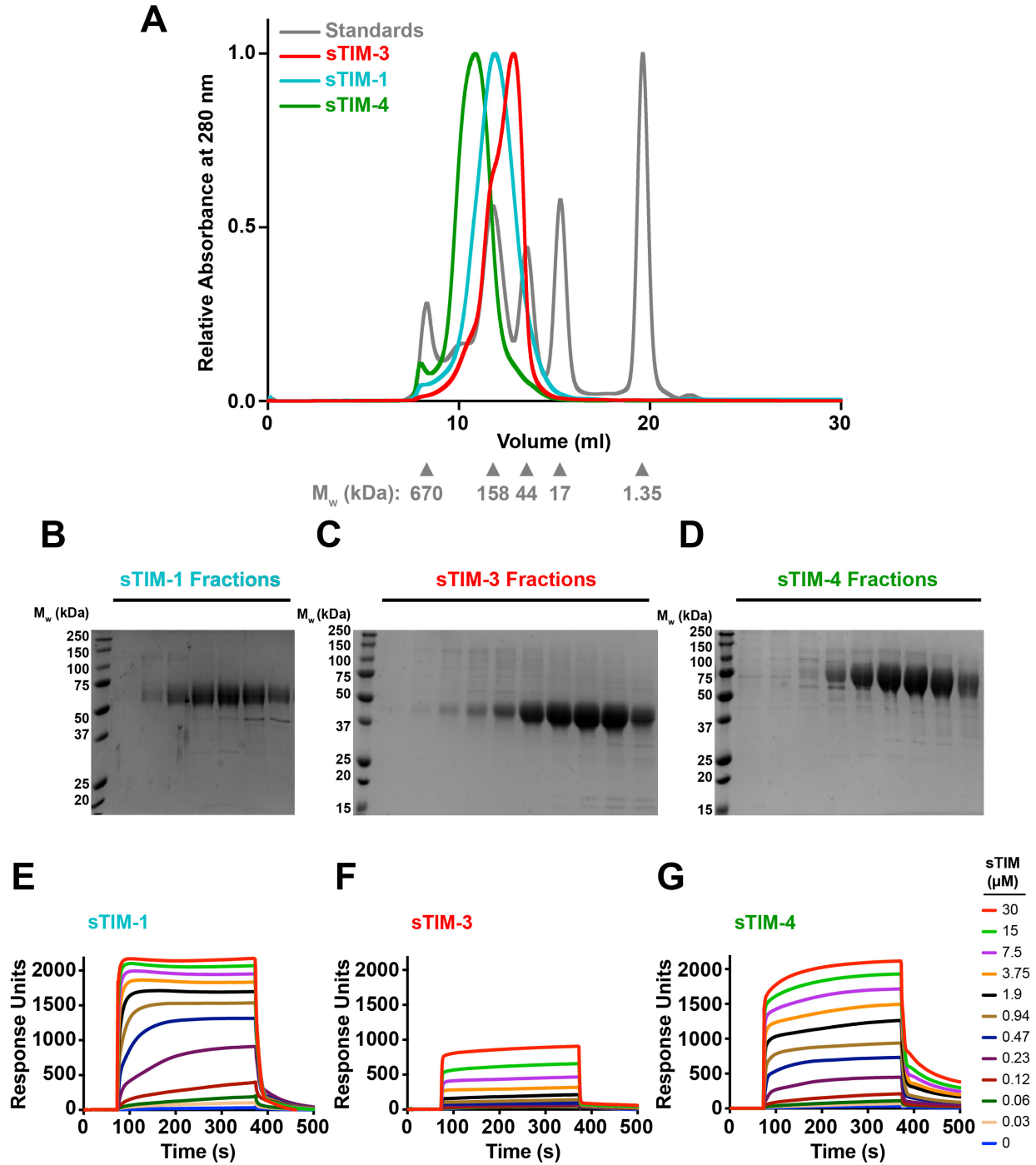


FIGURE S6: sTIM proteins are soluble and do not aggregate on the lipid surface

(A) Representative elution profiles of sTIM-1 (teal), sTIM-3 (red), and sTIM-4 (green) from a Superose 12 SEC column. An elution profile of protein molecular weight standards is shown in gray, with the corresponding molecular weights noted with gray arrowheads beneath the x-axis. (B-D) Representative SDS-PAGE analysis with Coomassie staining of SEC peak fractions for (B) sTIM-1, (C) sTIM-3, and (D) sTIM-4 eluted from the Superose 12 column, indicating that each protein is substantially pure, and runs as a reasonably monodisperse species in SEC.

(E-G) Representative sensorgrams of (E) sTIM-1, (F) sTIM-3, and (G) sTIM-4 binding to lipid membranes containing 20% PS in a PS background with 1 mM CaCl₂, with the corresponding binding curve shown in **Figure 4C**. A rapid increase in response is observed upon injection of protein solution over ~75 s, and signal returns to baseline at the end of the 300 s injection. Regeneration was performed with a NaOH wash between each cycle. The legend to the right of the figure indicates the protein concentration for each injection cycle (coded by color).

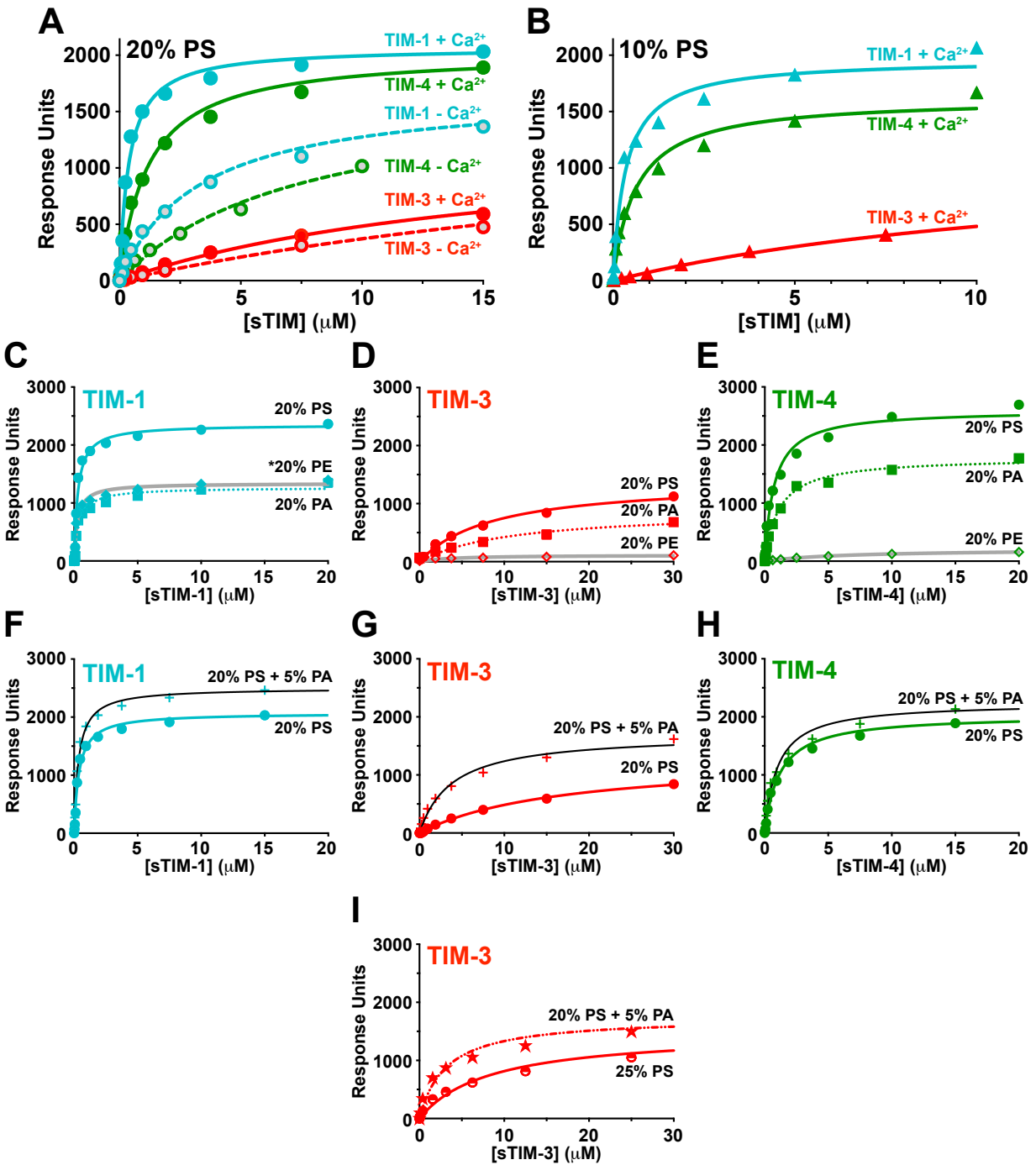


FIGURE S7: Phospholipid-binding characteristics of human TIMs

(A) Comparison of PS binding by sTIM-1 (teal), sTIM-3 (red), and sTIM-4 (green) with- and without 1 mM CaCl₂, assessed using SPR by flowing purified TIM extracellular regions (ECRs) over lipid vesicles containing 20% DOPS/80% DOPC immobilized on an L1 chip. The curves represent fits of the data to a one-site specific binding equation in Prism 8. Mean K_d values and standard deviations are shown in Supplemental Table S1.

(B) sTIM protein binding to 10% DOPS/90% DOPC surface membranes was determined in the presence of 1 mM CaCl₂. Binding curves in this experiment are representative of at least 2 independent experiments, except for sTIM-1 (n=1).

(C-E) sTIM binding to 20% DOPS/80% DOPC (circles), 20% DOPA/80% DOPC (squares), or 20% DOPE/80% DOPC (diamonds) surface was determined in the presence of 1 mM CaCl₂ for sTIM-1 (teal), sTIM-3 (red), and sTIM-4 (green), with binding curves representative of at least 2 independent experiments, except for TIM-4. Note that all sTIMs bind PA significantly, but that sTIM-1 is unique in also binding substantially to PE as described in the text (gray line in C).

(F-H) sTIM binding to 20% DOPS/80% DOPC (circles) or 20% DOPS/5%DOPA/75% DOPC (crosses) surface was determined in the presence of 1 mM CaCl₂. For each sTIM protein, adding 5% PA (mole/mole) detectably increases binding.

(I) sTIM-3 binding to 20% DOPS/5% PA/75% DOPC (stars) surface was determined in the presence of 1 mM CaCl₂, and found to exceed that seen for 25% DOPS/75% DOPC (half-filled circles), indicating some preference for PA.

TABLE S1. SPR Data for TIM family members binding to PS-containing membranes.

% PS	Sample	CaCl₂ (mM)	K_{d,app} ± Std. Dev (μM)	N
	sTIM-1	1	0.49	1
10%	sTIM-3	1	22.4 ± 12.6	6
	sTIM-4	1	0.69 ± 0.05	2
	sTIM-1	0	3.13 ± 0.31	2
20 %	sTIM-3	0	20.4 ± 10.5	3
	sTIM-4	0	7.21 ± 0.45	2
	sTIM-1	1	0.35 ± 0.05	6
20%	sTIM-3	1	9.70 ± 4.20	11
	sTIM-4	1	0.77 ± 0.32	5
	sTIM-1	1	0.35	1
20 % + 5 % PA	sTIM-3	1	3.45 ± 0.49	2
	sTIM-4	1	1.00	1